KASTAMONU ÜNİVERSİTESİ
2006

INOTECH

Inspiring Technologies and Innovations

Kastamonu Üniversitesi
TEKNOLOJİ TRANSFER OFİSİ

June
2024

E-ISSN : 2822-6062

Volume : 3 Issue : 1

KASTAMONU ÜNİVERSİTESİ 2006

Kastamonu Üniversitesi TEKNOLOJİ TRANSFER OFİSİ

INOTECH

Inspiring Technologies and Innovations Journal

E-ISSN: 2822-6062

Volume 3 Issue 1
June 2024

Preface

The publication process of the ‘Inspiring Technologies and Innovations (INOTECH)’ journal is continuing with the decision numbered 261 taken at the session of the Senate of Kastamonu University dated 2.12.2021 and numbered 26, and with the coordination of Kastamonu University Technology Transfer Office.

Our journal named ‘Inspiring Technologies and Innovations (INOTECH), which is a pioneer because it prioritizes R&D and innovation issues in multidisciplinary fields, is a peer-reviewed, open access, free publication policy and periodical research journal by Kastamonu University twice a year.

Aiming to develop in the way of presenting qualified works to national and international readers with the principle of scientific publishing, this first issue of our journal includes 5 original research and 1 review research articles from different disciplines and research fields.

We would like to thank all the academicians who contributed by sending their works, and all the referees who contributed in the evaluation process of these works;

We hope that the interest and support for our journal from the national and international community
will increase.

Regards.

Prof. Dr. Kasım YENİGÜN
Chief Editor

Inspiring Technologies and Innovations

Volume 3 / Issue 1 / 2024

Mail Adress:
Kastamonu Üniversitesi Rektörlüğü
Kuzeykent Mahallesi Orgeneral Atilla Ateş Paşa Caddesi No: 19
Kuzeykent/KASTAMONU
Posta Kodu: 37150 KASTAMONU/TÜRKİYE

inotech@kastamonu.edu.tr

Content

Volume 3 / Issue 1 / 2024

INO TECH Inspiring Technologies and Innovations

Inspiring Technologies and Innovations

June 2024, Volume: 3 Issue: 1

Research Article

Spatiotemporal Modeling and Simulation of DC Microplasma Glow Discharges in the ZnSe-Ar/H_2 System

Erhan ONGUN[a], Hatice Hilal YÜCEL (KURT)[b]

[a,b]Gazi University, Graduate School of Natural and Applied Sciences, Department of Physics, TÜRKİYE.

ORCID[a]: 0009-0007-4966-1044
ORCID[b]: 0000-0002-1277-5204

Corresponding Author e-mail: hkurt@gazi.edu.tr
https://doi.org/10.5281/zenodo.12544420

Received	: 25.12.2023	Accepted	: 19.04.2024	Pages	: 01-08

ABSTRACT: With their unique electrical and optical properties, microplasmas have become the focus of great interest in the broad field of plasma science and engineering in designing advanced materials and devices, including light sources, photodetectors, and microplasma field effect transistors. This conceptual research study was carried out for the numerical analyzes of gas discharge-semiconductor microplasma (GDSμP) systems in the COMSOL Multiphysics program. Plasma modeling was based on the electron energy distribution using Maxwell analytic function. Zinc selenide (ZnSe), a type II-VI compound semiconductor, was modeled as the cathode electrode with a micro-digitated electron emission surface, coupled to a micro discharge gap of unary argon (Ar) and binary argon/hydrogen (Ar/H_2) gases. Bandgap tunable ZnSe has attracted the attention of researchers for various optoelectronic applications, including high-efficiency and fast-response infrared imaging devices in the near-to-mid infrared spectrum. The binary gas system consisted of argon mixed with 10% molar hydrogen. Spatiotemporal distribution patterns of the main discharge parameters were plotted across 100 μm long discharge gap of a two-dimensional square chamber in gases media at 250 Torr sub atmospheric pressure. Microscale normal glow discharges were generated under electric field fed with a constant voltage of 1300 VDC in a virtual electrical equivalent circuit (EEC). GDSμP cells were simulated to explore the fast transient discharge parameters, including electron density (ED), electron current density (ECD), and electric potential (EP). It was figured out that microplasma devices combined with gas discharge-semiconductor systems can be specifically designed for infrared detector and image converter applications.

KEYWORDS: Microplasma, zinc selenide, glow discharge, simulation, infrared, image converter.

1. INTRODUCTION

The area of microplasma has become a focus of increasing interest in the plasma science and technology. Microplasmas are non-thermal, high-energy-density and non-equilibrium reactive gas discharge media that feature at least one physical dimension in the micrometer range. Their unique electrical and optical characteristics make microplasmas attractive for designing novel materials and functional devices in various applications, including light sources, photodetectors, and microplasma field effect transistors. Microplasmas are generated by electrical breakdown in gases at sub atmospheric or atmospheric pressures.

A topical review published in the field of microplasma science and technology provided a comprehensive status report into the microplasma research with examples of applications [1]. Recent research works were also reported in the field of microplasma device technology [2,3]. Several theoretical and experimental investigations were reported in the gas discharge-semiconductor microplasma systems (GDSμP) [4]. Direct-current (DC) argon (Ar) glow discharges were experimentally investigated for infrared-to-visible wavelength conversion applications. Nonlinear electrical transport properties were reported for Ar -glow discharges over a wide range of sub atmospheric pressures under various infrared (IR) light illumination intensities on gallium arsenide (GaAs) semiconductor cathode electrode [5,16]. Electron emission mechanisms on microscale gas breakdown were extensively reported [6,7]. The Townsend avalanche governs the ionization process for gases, in which thermofield emission, ion-induced secondary electron emission, and field emission mechanisms are involved. The phenomenon of gas breakdown has also been studied using computational methods [8].

Zinc selenide (ZnSe), a type II-VI compound semiconductor, is a unique bandgap tunable semiconductor material with excellent electronic transport properties and optical transparency in the visible spectrum. ZnSe -based optoelectronic device applications were reviewed in [9,10]. The infrared sensitivity of ZnSe was specifically investigated for the infrared-to-visible conversion device applications [11]. DC -driven Ar -glow discharges in microgaps combined with ZnSe cathode were experimentally explored under atmospheric pressures [12]. The electrical discharge parameters in the ZnSe-Ar/H_2 system were investigated numerically and experimentally at sub atmospheric pressures under infrared illumination [13].

The effect of cathode surface morphology, including intrinsic surface roughness and artificial surface patterning, such as the growth of multiple concentric protrusions, on electron emission mechanisms was examined [14,15].

Figure 1 shows the schematic representation of GDSS cell for the infrared-to-visible wavelength conversion device application.

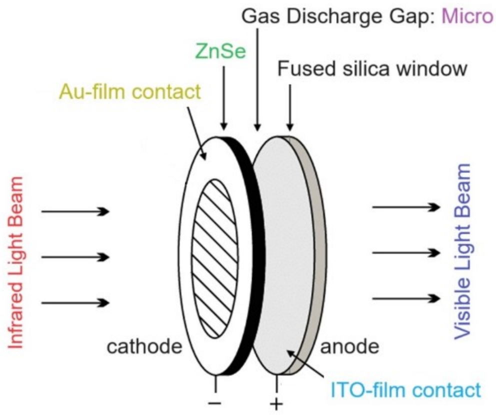

Figure 1. Sketch of GDSS cell, intended for infared-to-visible wavelength conversion application.

2. MATERIAL AND METHOD

The gas discharge-semiconductor microplasma (GDSµP) system was modeled and simulated in 2D media. The surface of the semiconductor cathode electrode, exposed to infrared (IR) light beam, was coated with thin gold (Au) film as electrical contact element. The surface of the fused-glass substrate of the anode electrode, exposed to glow light emissions (GLE), was coated with thin ITO film as electrical contact element.

Type II-VI compound semiconductor zinc selenide (ZnSe) as the cathode material was modeled in comb-plate style with micro-digitated electron emission surface, coupled to a micro discharge gap of unary argon (Ar) and binary argon/hydrogen (Ar/H_2) gases. The binary gas system consisted of Ar mixed with 10% molar H_2 gas. A two-dimensional square chamber with 100 µm long discharge gap was introduced in unary Ar and binary Ar/H_2 gases at 250 Torr sub atmospheric pressure. Microscale normal glow discharges were generated under electric field fed with a constant voltage of 1300 VDC in a virtual electrical equivalent circuit (EEC) in the simulation platform.

Numerical analyzes of gas discharge-semiconductor microplasma (GDSµP) systems were performed in the COMSOL Multiphysics program using the electron energy distribution function. Microplasma simulations were run to explore the fast transient discharge parameters, including electron density (ED), electron current density (ECD), and electric potential (EP). The variables in the GDSµP system simulation runs are tabulated in Table 1.

Table 1. The variables in the GDSµP system simulation runs.

Parameter	**Value/Description**
Voltage between electrodes (anode-to-cathode)	V = 1300 VDC
Gas types	Ar and Ar/H_2 (10%)
Gas pressure	P = 250 Torr
Distance between electrodes (anode-to-cathode)	d = 100 µm
Cathode electrode material type	ZnSe with micro-digitated surface
Cathode electrode diameter	D = 100 µm
Anode electrode material type	ITO-film coated SiO_2 window
Density of initial (seed) electrons in the gas discharge medium	$n_{e,o}$ = 1E17 (1/m^3)
Paschen product	P.d = 2.5 Torr.cm
Ambient operating temperature of GDSµP cell	T = 300 K

The physical and mesh structures of GDSµP cell model are shown in Figure 2.

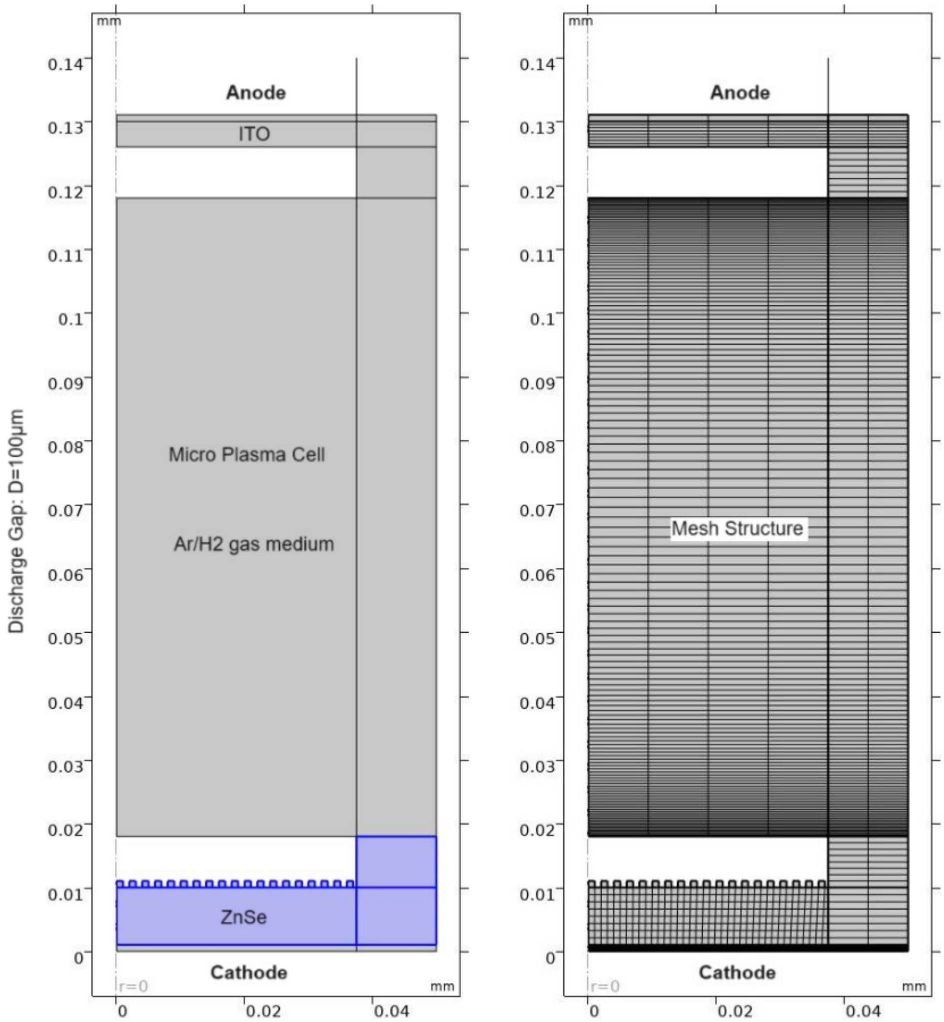

Figure 2. Sketch of GDSµP cell model in 2D layout: (a) Physical structure, and (b) Mesh structure.

3. RESULTS

In Figure 3, the spatiotemporal distributions of the electron density (ED) parameter data obtained across 100 µm long discharge gap were plotted as curves, respectively for; (a) initial phase of unary Ar -system, (b) initial phase of binary Ar/H_2 -system, (c) final phase of unary Ar -system, (d) final phase of binary Ar/H_2 -system, (e) full period of unary Ar -system, and (f) full period of binary Ar/H_2 -system.

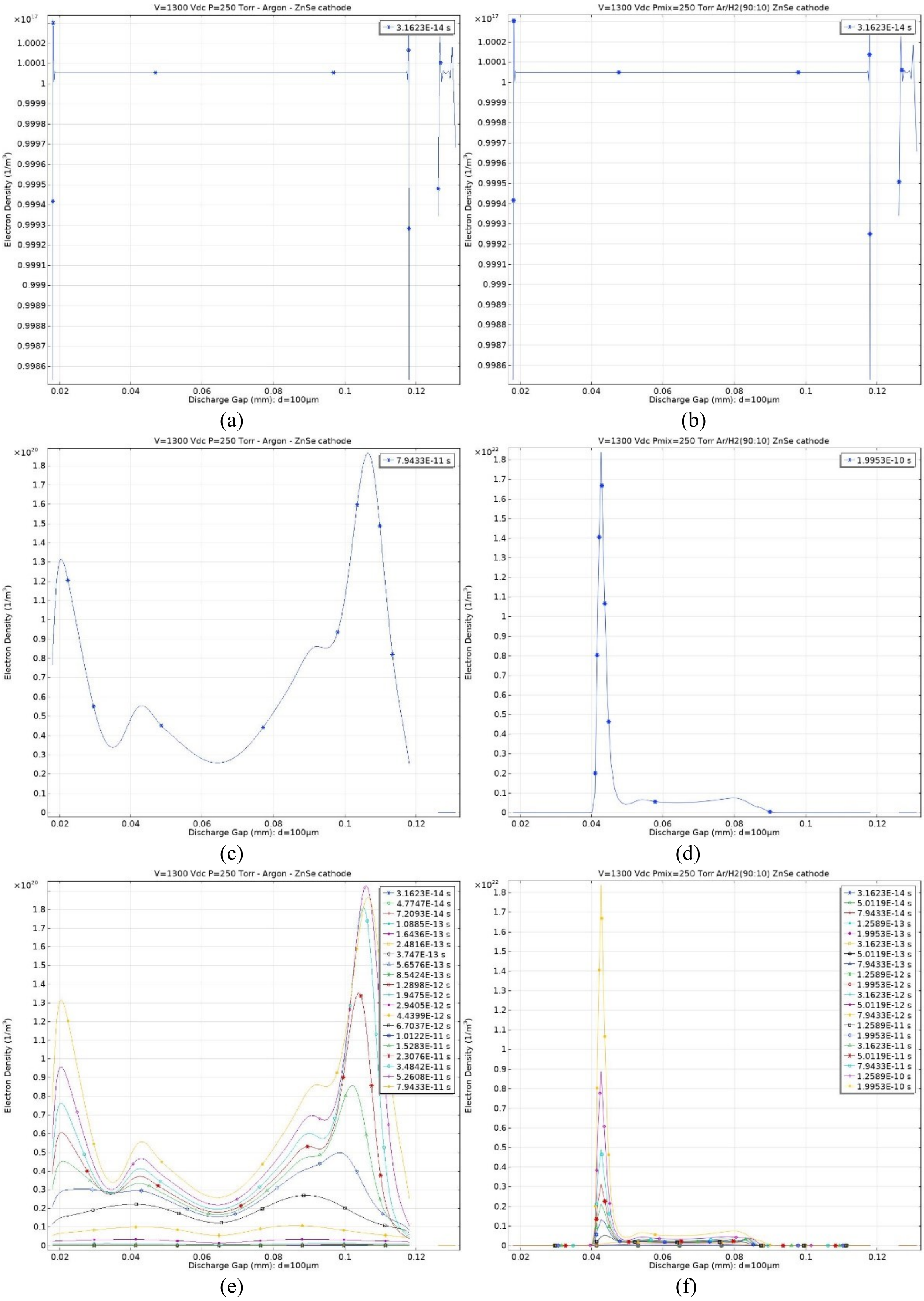

Figure 3. Spatiotemporal distributions of electron density (ED) data across 100 µm long discharge gap, respectively for; (a) initial phase of unary Ar -system, (b) initial phase of binary Ar/H_2(90:10) -system, (c) final phase of unary Ar -system, (d) final phase of binary Ar/H_2 (90:10) -system, (e) full period of unary Ar -system, (f) full period of binary Ar/H_2 (90:10) -system.

In Figure 4, the spatial distributions of the electron density (ED) parameter data obtained across 100 µm long discharge gap are shown in 3D images, respectively for; (a) final phase of unary Ar -system, and (b) final phase of binary Ar/H_2 (90:10) -system.

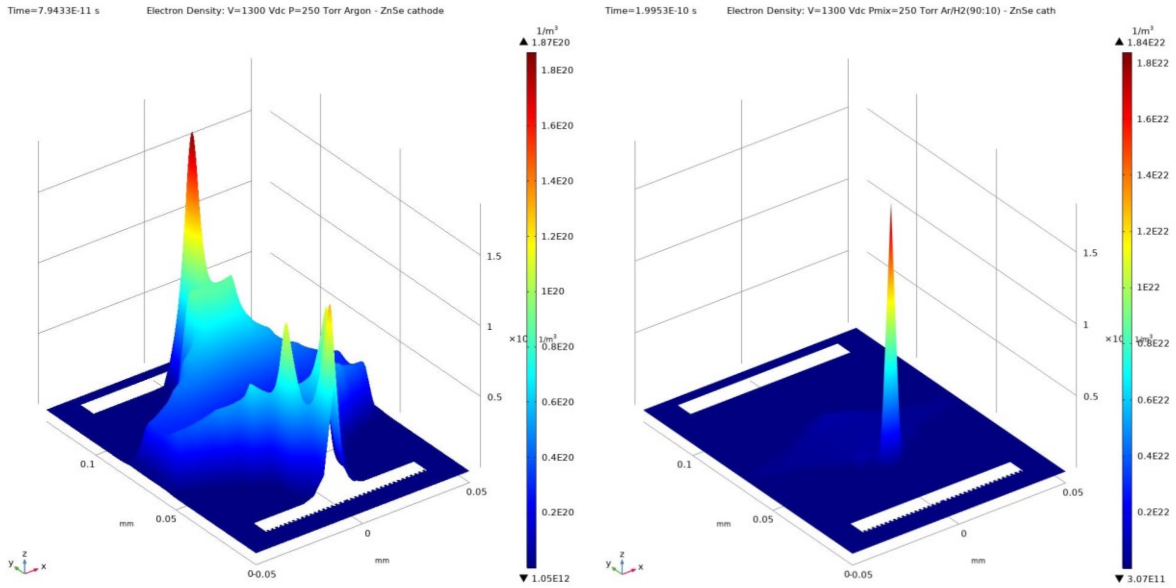

(a) (b)

Figure 4. Spatial distributions of electron density (ED) data obtained across 100 µm long discharge gap in 3D images, respectively for; (a) final phase of unary Ar -system, (b) final phase of binary Ar/H_2 (90:10) -system.

In Figure 5, the spatial distributions of the electron current density (ECD) parameter data obtained across 100 µm long discharge gap are shown in 3D images, respectively for; (a) final phase of unary Ar -system, and (b) final phase of binary Ar/H_2 (90:10) -system.

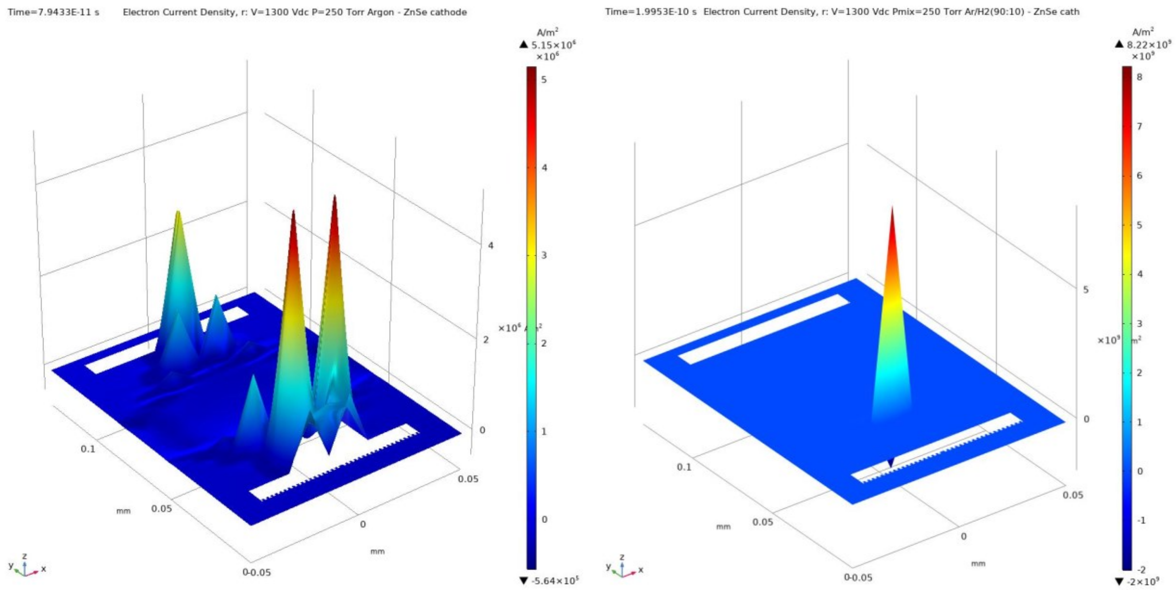

(a) (b)

Figure 5. Spatial distributions of electron current density (ECD) data obtained across 100 µm long discharge gap in 3D images, respectively for; (a) final phase of unary Ar -system, (b) final phase of binary Ar/H_2 (90:10) -system.

In Figure 6, the spatial distributions of the electric potential (EP) parameter data obtained across 100 µm long discharge gap are shown in 3D images, respectively for; (a) final phase of unary Ar -system, and (b) final phase of binary Ar/H_2 (90:10) -system.

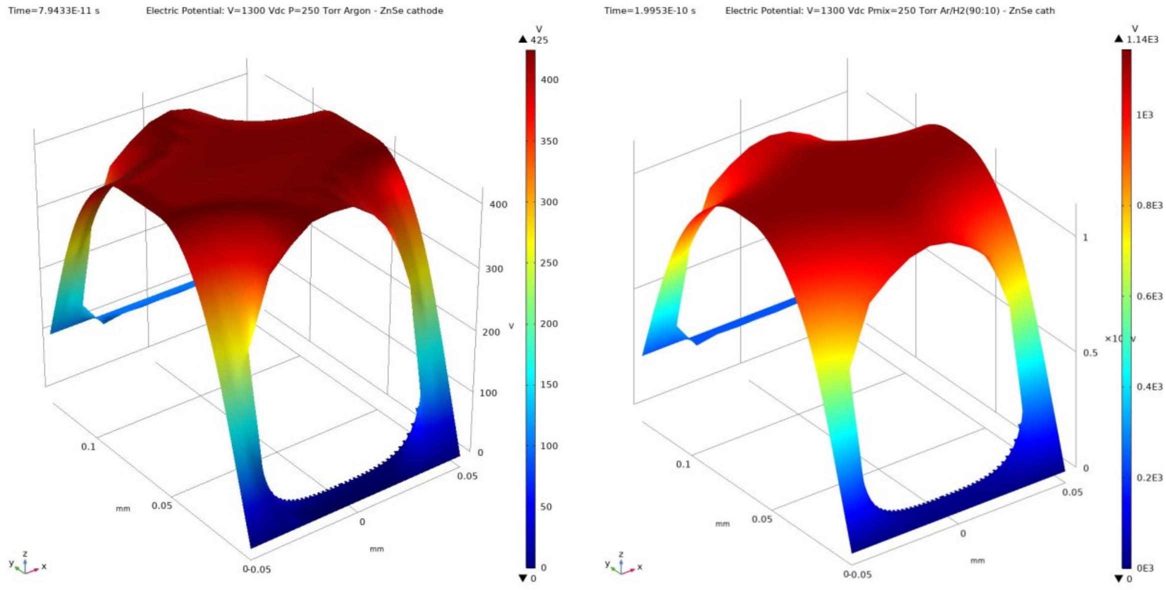

(a) (b)

Figure 6. Spatial distributions of electric potential (EP) data obtained across 100 μm long discharge gap in 3D images, respectively for; (a) final phase of unary Ar -system, (b) final phase of binary Ar/H_2 (90:10) -system.

Table 2 summarizes the comparative data of discharge parameters, including electron density, electron current density, and electric potential for unary Ar and binary Ar/H_2 (90:10) -systems.

Table 2. Comparative data of discharge parameters: Unary argon (Ar) and binary argon/hydrogen (Ar/H_2) -systems.

Parameter	Unary Ar -system	Binary Ar/H_2 (90:10) -system
SS_o	Simulation run started at time (s):	
	$3.1623x10^{-14}$	$3.1623x10^{-14}$
SS_f	Simulation run ended at time (s):	
	$7.9433x10^{-11}$	$1.9953x10^{-10}$
$ED_{i,0}$	Initial Electron Density ($1/m^3$):	
	$1.0x10^{17}$	$1.0x10^{17}$
$ED_{f,p}$	Electron Density at the final phase, peak ($1/m^3$):	
	$1.87x10^{20}$	$1.84x10^{22}$
$ECD_{f,p}$	Electron Current Density at the final phase, peak (A/m^2):	
	$5.15x10^6$	$8.22x10^9$
$EP_{f,p}$	Electric Potential at the final phase, peak (V):	
	425	1140

According to the numerical analyzes conducted within the scope of this study;

Referring to the data summarized in Table 2 for unary Ar and binary Ar/H_2 (90:10) -systems of the proposed GDSμP simulation model, the following comparative results were obtained:

- Simulation runs of unary Ar and binary Ar/H_2 -systems were started at the same time in seconds; SS_o.
- Binary Ar/H_2 -system stabilized slightly longer in time than unary Ar -system; SS_f.
- Initial electron density value was set the same for both unary Ar and binary Ar/H_2 -systems; $ED_{i,0}$.
- Peak electron density value at the final phase of the discharge period for binary Ar/H_2 -system was 100 times higher than that for unary Ar -system, $ED_{f,p}$.
- Peak electron current density value at the final phase of the discharge period for binary Ar/H_2 -system was 1000 times higher than that for unary Ar -system, $ECD_{f,p}$.

- Peak electric potential value at the final phase of the discharge period for binary Ar/H_2 -system was 1140 VDC, higher than that for unary Ar -system 425 VDC, $EP_{f,p}$.

In Figure 7, the Paschen curves are shown for argon and hydrogen gas discharges [3]. The static breakdown voltage (V_B) of a gas medium is defined by the product of gas pressure (***P***, Torr) and inter-electrode gap distance (***d***, cm), corresponding to ***P.d*** in Torr.cm. In this study, the ***P.d*** product corresponding to 2.5 Torr.cm is marked by the vertical dot line on the Paschen curves of argon and hydrogen gasses.

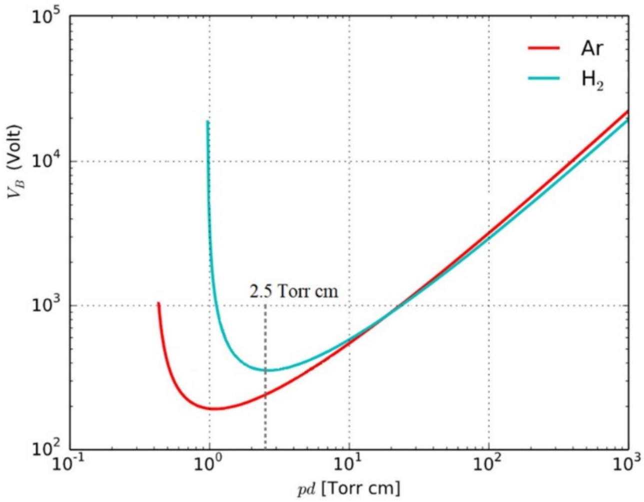

Figure 7. The ***P.d*** product corresponding to 2.5 Torr.cm, marked on the Paschen curves of Ar and H_2 gasses [3].

In Figure 8, the voltage-current (V-I) curve for a typical gas discharge system is shown [13]. The peak discharge currents of the simulation runs were estimated to be approximately 0.5 mA for unary Ar -system and 10 mA for binary Ar/H_2 -system, lying in the normal glow discharge regime of the V-I curve.

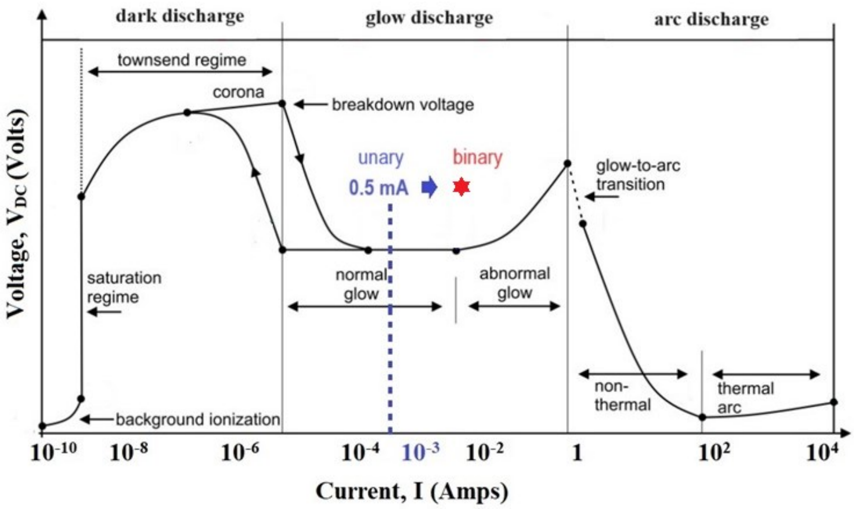

Figure 8. Peak discharge currents of unary Ar and binary Ar/H_2 -discharge systems, lying in the normal glow discharge regime of the V-I curve [13].

By adding hydrogen to argon, forming binary Ar/H_2 -system, the calculated peak discharge current was located in the upper part of the normal glow discharge region, which theoretically did not extend to the abnormal glow discharge region for the electrical stability of the semiconductor-gas discharge microplasma system.

4. CONCLUSION

The spatiotemporal distributions of the electron density and the electron current density parameters in binary Ar/H_2 -system were locally more concentrated and numerically stronger than in unary Ar -system as discharge reactions progressed over the discharge period. The peak electron density value at the final phase of the discharge period for binary Ar/H_2 -system was 100 times higher than that for unary Ar -system. The peak electron current density value at the final phase of the discharge period for binary Ar/H_2 -system was 1000 times higher than that for unary Ar -system.

It was revealed that by adding hydrogen to argon, the electrical stability of ZnSe cathode material and the spatiotemporal distribution uniformity of glow-discharge emissions were enhanced over the discharge period of the fast-transient microplasma reactions. The safe operating voltage of a microplasma device for a given microgap can be precisely tuned on the Paschen curve by adding hydrogen at an appropriate molar fraction to argon at a well-defined pressure level. It was figured out that gas discharge-semiconductor microplasma (GDSµP) systems can be specifically designed for the infrared detector and image converter device applications.

ACKNOWLEDGEMENT

The Scientific Research Projects Coordination Unit of Gazi University supported this study with the project number FDK-2023-8704.

ETHICAL STANDARD DECLARATION

It was declared by the authors that the materials and methods used in this article do not require any ethics committee permission.

AUTHORS' CONTRIBUTIONS

Erhan ONGUN: Modeling, numerical analysis, article writing.
Prof. Dr. Hatice Hilal YÜCEL (KURT) : Supervisor of EO's doctoral thesis, expert on the plasma science and technology, numerical analyses, article writing and editing.

CONFLICT OF INTEREST

There is no conflict of interest in this study.

DATA AVAILABILITY STATEMENT

The supplementary data for this article can be requested from the corresponding author.

REFERENCES

[1] Schoenbach, K.H., Becker, K. (2016). 20 years of microplasma research: A status report. *Eur. Phys. J. D*, 70, 29.
[2] Chiang, W.-H., Mariotti, D., Sankaran, R.M., Eden, J.G., Ostrikov, K. (2020). Microplasmas for advanced materials and devices. *Adv. Mater.*, 32, 1905508.
[3] Azar, M.T., Pai, P. (2017). Microplasma field effect transistors. *Micromachines*, 8(4), 117.
[4] Kurt, H.H., Koc, E., Salamov, B. (2010). Atmospheric pressure DC glow discharge in semiconductor gas discharge electronic devices. *IEEE Transactions on Plasma Science*, 38(2), 137.
[5] Sadiq, Y., Kurt, H.Y., Albarzanji, A.O., Alekperov, S.D., Salamov, B.G. (2009). Transport properties in semiconductor-gas discharge electronic devices. *Solid-state electronics*, 53(9), 1009.
[6] Garner, A.L., Meng, G., Fu, Y., Loveless, A.M., Brayfield II, R.S., Darr, A.M. (2020). Transitions between electron emission and gas breakdown mechanisms across length and pressure scales. *J. Appl. Phys.*, 128, 210903.
[7] Go, D.B., Venkattraman, A. (2014). Microscale gas breakdown: ion-enhanced field emission and the modified Paschen's curve. *J. Phys. D: Appl. Phys.*, 47, 503001.
[8] Garner, A.L., Loveless, A.M., Dahal, J.N., Venkattraman, A. (2020). A tutorial on theoretical and computational techniques for gas breakdown in microscale gaps. *IEEE Transactions on Plasma Science*, 99:1-17.
[9] Donald, D.H., Hendrik, C.S., Setumo, V.M., Lehlohonolo, F.K. (2022). *Zinc selenide semiconductor: synthesis, properties and applications. Nanoscale Compound Semiconductors and their Optoelectronics Applications*, Woodhead Publishing Series in Electronic and Optical Materials, 67-84. https://doi.org/10.1016/B978-0-12-824062-5.00001-4.
[10] Morkoc, B.H., Strite, S., Gao, G.B., Lin, M.E., Sverdlov, B., Burns, M. (1994). Large-band-gap SiC, III-V nitride, and II-VI ZnSe-based semiconductor device Technologies. *Journal of Applied Physics*, 76(3), 1363.
[11] Kurt, H.H., Tanrıverdi E. (2017). Electrical Properties of ZnS and ZnSe Semiconductors in a plasma-semiconductor system. *Journal of Electronic Materials*, 46(7), 3965.
[12] Kurt, H.H. (2018). Exploration of gas discharges with GaAs, GaP and ZnSe electrodes under atmospheric pressure. *Journal of Electronic Materials*, 47, 4444.
[13] Ongun, E., Yücel (Kurt), H.H., Utaş, S. (2024). DC-driven subatmospheric glow discharges in the infrared-stimulated. *J Mater Sci: Mater Electron*, 35:655, https://doi.org/10.1007/s10854-024-12382-1.
[14] Brayfield II, R.S., Fairbanks, A.J., Loveless, A.M., Gao, S., Dhanabal, A., Li, W., Darr, C., Wu, W., Garner, A.L. (2019). The impact of cathode surface roughness and multiple breakdown events on microscale gas breakdown at atmospheric pressure. *J. Appl. Phys.*, 125, 203302.
[15] Fu, Y., Zhang, P., Krek, J., Verboncoeur, J.P. (2019). Gas breakdown and its scaling law in microgaps with multiple concentric cathode protrusions. *Appl. Phys. Lett.*, 114, 014102.
[16] Kurt, H.Y., İnaloz A., Salamov, B.G. (2010). Study of non-thermal plasma discharge in semiconductor gas discharge electronic devices. *Optoelectronics and Advanced Materials-Rapid Communications*, 4, 205.

INO TECH Inspiring Technologies and Innovations

Inspiring Technologies and Innovations

June 2024, Volume: 3 Issue: 1

Research Article

Parameter Estimation of PV Solar Cells and Modules using Metaheuristic Optimization Algorithm

Rafa Elshara[a] Aybaba Hançerlioğullari[b]

[a] Department of Material Science and Engineering, University of Kastamonu, Kastamonu 37150, TÜRKİYE.
[b] Department of Physics, Science Faculty, University of Kastamonu, Kastamonu 37150, TÜRKİYE.

ORCID[a]: 0000-0003-4078-3735
ORCID[b]: 0000-0002-9830-4226

Corresponding Author e-mail: roamer29@mail.com
https://doi.org/10.5281/zenodo.12597777

Received : 07.03.2024 Accepted : 29.06.2024 Pages : 09-16

ABSTRACT: Photovoltaic (PV) solar cells and modules are crucial components of renewable energy systems, necessitating accurate parameter estimation for optimal performance and efficiency. This paper proposes the utilization of the Grasshopper Optimization Algorithm (GOA) for parameter estimation in PV solar cells and modules. The proposed methodology aims to enhance the accuracy and efficiency of parameter estimation by leveraging the unique search mechanism of the GOA, which mimics the foraging behavior of grasshoppers in nature. Through iterative optimization, the GOA efficiently explores the solution space to identify optimal parameters that best fit experimental data, such as current-voltage (IV) and power-voltage (PV) characteristics. The paper provides a comprehensive overview of the parameter estimation process, detailing the formulation of the objective function to minimize the error between experimental and simulated data. Furthermore, it discusses the implementation of the GOA algorithm and its integration with mathematical models of PV solar cells and modules. To validate the effectiveness of the proposed approach, experimental data from real-world PV systems are utilized. Comparative analyses with other optimization algorithms demonstrate the superior performance of the GOA in terms of convergence speed and accuracy in parameter estimation. The results indicate that the proposed methodology offers a robust and efficient solution for parameter estimation in PV solar cells and modules, thereby facilitating the design, optimization, and maintenance of photovoltaic systems. The integration of the GOA algorithm contributes to advancing the state-of-the-art in renewable energy technologies, promoting the widespread adoption of solar power generation for sustainable development. The proposed algorithm significantly outperforms all competitors in SMD, with WOA being the closest but still 26.1% worse. While GWO performs well in DDM, it still lags behind the suggested method by 31.7%. Although achieving comparable results to COA in PV, the proposed algorithm maintains an edge with COA trailing by 4.2%.

KEYWORDS: Photovoltaic Solar Cells, Metaheuristic Optimization Algorithm, Parameter Estimation.

1. INTRODUCTION

The rapid depletion of fossil fuel reserves and growing concerns regarding environmental degradation have led to an increased focus on renewable energy sources, with solar power emerging as a prominent candidate for sustainable electricity generation. Among various solar technologies, photovoltaic (PV) cells and modules play a pivotal role in harnessing solar energy and converting it into usable electricity. However, to ensure optimal performance and efficiency of PV systems, accurate parameter estimation of solar cells and modules is indispensable [1], [2].

Parameter estimation involves determining the key electrical parameters of PV devices, such as the ideality factor, series and shunt resistances, and photocurrent, which significantly influence their behavior under different operating conditions. Precise estimation of these parameters is essential for designing efficient PV systems, predicting their performance, and optimizing their operation. Traditional methods for parameter estimation often rely on iterative numerical techniques, which may suffer from computational inefficiencies and convergence issues, particularly when dealing with complex models and experimental data [3], [4].

To address these challenges, this paper introduces a novel approach for parameter estimation of PV solar cells and modules utilizing the Grasshopper Optimization Algorithm (GOA). The GOA is a metaheuristic optimization technique inspired by the natural foraging behavior of grasshoppers, which has demonstrated remarkable efficiency and robustness in solving complex optimization problems across various domains [5].

The primary objective of this study is to leverage the unique search mechanism of the GOA to enhance the accuracy and efficiency of parameter estimation in PV devices. By formulating an appropriate objective function to minimize the error between experimental and simulated data, the proposed methodology aims to identify the optimal set of parameters that best represent the behavior of solar cells and modules under different operating conditions [6].

In this introduction, we provide an overview of the significance of parameter estimation in PV technology and highlight the limitations of existing methods. Subsequently, we introduce the Grasshopper Optimization Algorithm and its potential applicability to the parameter estimation problem in PV solar cells and modules. Furthermore, we outline the structure of the paper, including the methodology, experimental setup, results, and discussion sections, to provide a comprehensive understanding of the proposed approach and its implications for renewable energy research and practice.

1.1. Contribution

The novel application of the Grasshopper Optimization Algorithm (GOA) for parameter estimation in PV solar cells and modules is a significant contribution to the field of renewable energy. By leveraging the unique search mechanism inspired by grasshopper foraging behavior, this methodology introduces a fresh perspective on optimizing PV system parameters. This innovative approach offers a new tool for researchers and practitioners to enhance the accuracy and efficiency of parameter estimation in photovoltaic systems.

1.2. Originality

The integration of the GOA algorithm with mathematical models of PV solar cells and modules represents an original and innovative strategy for parameter estimation. The systematic examination of the parameter estimation process, including the formulation of an objective function to minimize discrepancies between experimental and simulated data, demonstrates a rigorous approach to addressing challenges in accurate parameter estimation. This original methodology pushes the boundaries of current knowledge by providing a clear roadmap for researchers to follow in optimizing PV systems using nature-inspired meta-heuristic algorithms.

The study organization provides a brief outline of the content in each section. Section 2 reviews the literature, Section 3 describes the materials and methods, Section 4 presents the results and discussion, and Section 5 provides the conclusion. This overview helps readers understand the structure of the study and anticipate the content of each section.

2. LITERATURE REVIEW

Photovoltaic (PV) solar cells and modules are critical components of renewable energy systems, driving the transition towards sustainable electricity generation. Effective parameter estimation of PV devices is essential for optimizing their performance, enhancing energy conversion efficiency, and facilitating the design and operation of solar power systems. In this section, existing literature on parameter estimation techniques for PV solar cells and modules is reviewed, with a focus on highlighting the challenges and opportunities in this field [7].

Traditional methods for parameter estimation in PV devices often rely on numerical techniques such as the iterative least squares method, Newton-Raphson method, and gradient descent algorithms. These methods involve iterative optimization procedures to minimize the error between experimental and simulated data. While effective in many cases, traditional methods may suffer from computational complexity, sensitivity to initialization, and convergence issues, particularly when dealing with non-linear models and noisy experimental data [8].

In recent years, metaheuristic optimization techniques have gained prominence for parameter estimation in PV solar cells and modules. Metaheuristic algorithms, inspired by natural phenomena and biological processes, offer robust and efficient solutions for optimization problems with complex search spaces. Genetic algorithms, particle swarm optimization, simulated annealing, and ant colony optimization are among the widely used metaheuristic techniques in the field of PV parameter estimation. These algorithms exhibit superior performance in terms of convergence speed, solution quality, and scalability compared to traditional methods [9].

The Grasshopper Optimization Algorithm (GOA) is a relatively new metaheuristic optimization technique inspired by the swarming behavior of grasshoppers. Introduced by Saremi et al. in 2017, GOA mimics the collective foraging behavior of grasshoppers to efficiently explore the solution space and identify optimal solutions. The algorithm employs a population-based approach where individual grasshoppers iteratively adjust their positions based on local and global information to converge toward the optimal solution. The unique characteristics of GOA, such as simplicity, versatility, and robustness, make it a promising candidate for parameter estimation in PV solar cells and modules [10].

Numerous studies have explored the application of metaheuristic optimization algorithms, including genetic algorithms, particle swarm optimization, and simulated annealing, for parameter estimation in PV devices. These studies have demonstrated the effectiveness of metaheuristic techniques in accurately estimating key parameters such as the ideality factor, series and shunt resistances, and photocurrent of solar cells and modules. However, further research is needed to investigate the performance of emerging metaheuristic algorithms like GOA in this domain [11]. Despite the extensive research on parameter estimation techniques for PV solar cells and modules, there remains a need for novel approaches that can overcome the limitations of existing methods. The utilization of the Grasshopper Optimization Algorithm (GOA) for parameter estimation in PV devices represents a promising research direction. By leveraging the unique search mechanism of GOA, this paper aims to enhance the accuracy and efficiency of parameter estimation, thereby contributing to the advancement of renewable energy technologies[12].

3. MATERIALS AND METHOD

The materials and methods described below provide a systematic approach for parameter estimation of PV solar cells and modules using the Grasshopper Optimization Algorithm. By following these steps, accurate and efficient estimation of model parameters can be achieved, facilitating the design and optimization of photovoltaic systems for sustainable energy generation. Refer to Figure 1 for a visual representation of these processes.

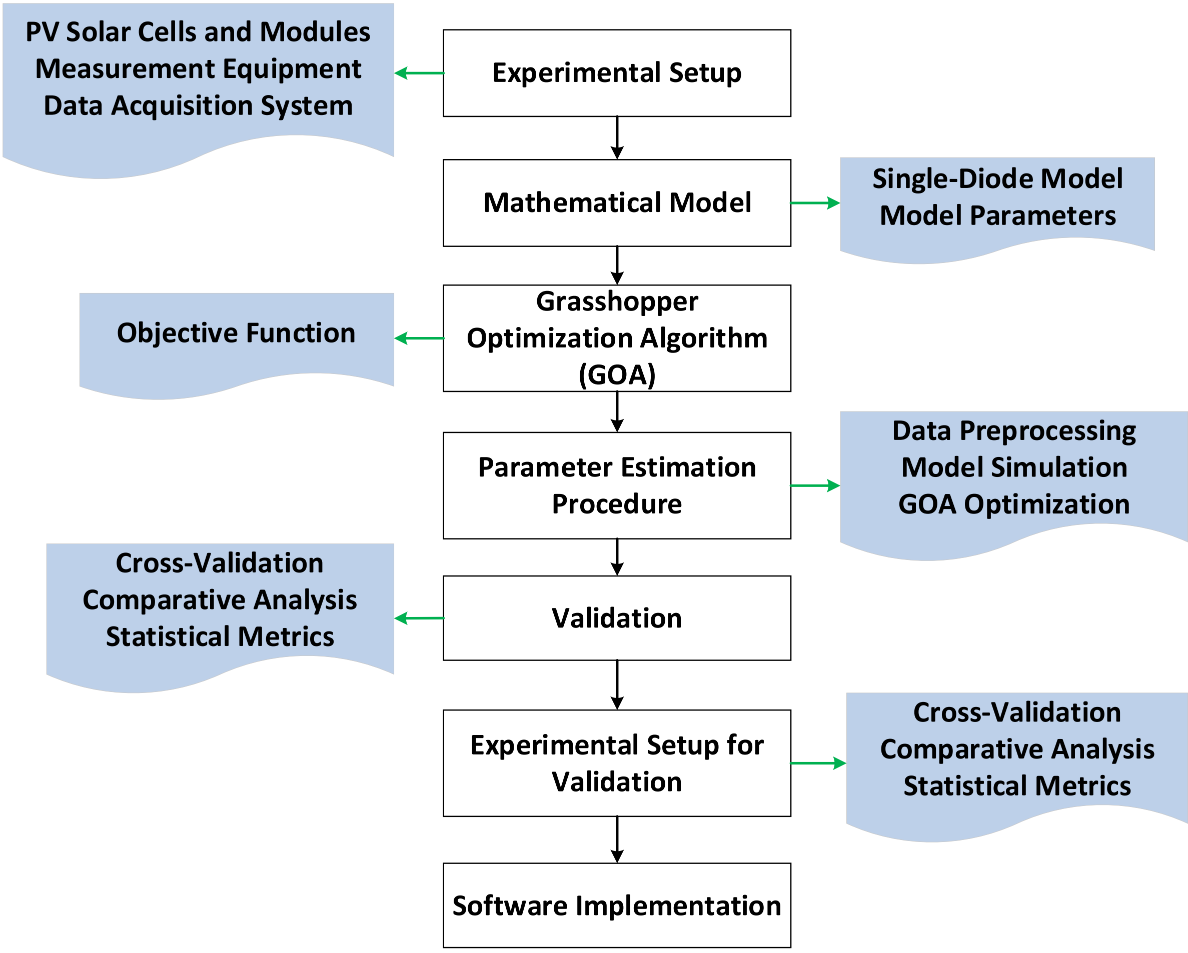

Figure 1. Grasshopper-based parameter extraction for PV module

a. Experimental Setup:

PV Solar Cells and Modules: Utilize commercially available PV solar cells and modules of known specifications.

Measurement Equipment: Employ high-precision instruments for measuring current-voltage (IV) characteristics, such as solar simulators and multimeters.

Data Acquisition System: Use a data acquisition system to capture experimental data, ensuring accuracy and reliability.

b. Mathematical Model:

Single-Diode Model: Adopt the widely used single-diode model to represent the electrical behavior of PV solar cells and modules.

Model Parameters: Define the parameters of the single-diode model, including the ideality factor, series and shunt resistances, photocurrent, and diode saturation current.

c. Grasshopper Optimization Algorithm (GOA):

Implementation: Implement the GOA algorithm using a suitable programming language or software platform.

Initialization: Initialize the population of grasshoppers with random solutions within predefined bounds.

Objective Function: Formulate the objective function to minimize the error between experimental and simulated IV characteristics.

Iterative Optimization: Conduct iterative optimization using the GOA to search for the optimal set of model parameters.

d. Parameter Estimation Procedure:

Experimental Data Collection: Measure IV characteristics of PV solar cells and modules under various operating conditions, including different irradiance levels and temperatures.

Data Preprocessing: Preprocess experimental data to remove noise and ensure consistency.

Model Simulation: Simulate the IV characteristics using the single-diode model with initial parameter estimates.

Objective Function Evaluation: Calculate the error between experimental and simulated IV characteristics using the formulated objective function.

GOA Optimization: Apply the GOA algorithm to minimize the objective function and update the model parameters iteratively.

Convergence Criterion: Define a convergence criterion to terminate the optimization process when a satisfactory solution is achieved.

e. Validation:

Cross-Validation: Validate the optimized model parameters using a separate dataset or cross-validation technique.

Comparative Analysis: Compare the performance of the GOA-based parameter estimation approach with other optimization algorithms, such as genetic algorithms or particle swarm optimization.

Statistical Metrics: Evaluate the accuracy and efficiency of the parameter estimation method using statistical metrics, such as root mean square error (RMSE) and coefficient of determination (R^2).

f. Experimental Setup for Validation:

Repeat the experimental setup described earlier for data collection using a separate set of PV solar cells and modules.

Implement the parameter estimation procedure with the GOA algorithm and compare the optimized parameters with reference values or results obtained using other optimization techniques.

g. Software Implementation:

Utilize appropriate software tools or programming languages for implementing the parameter estimation methodology and conducting simulations and optimizations.

Ensure compatibility and efficiency of the software implementation with the experimental setup and data analysis requirements.

3.1. Solar Cell Modeling and Parameter Identification

Solar cells are crucial in photovoltaic systems, transforming sunlight into electricity. To predict their performance and optimize their design, mathematical models are used. Among these models, the diode-based model is popular because it mimics the behavior of PV cells, which are made of semiconductor materials exhibiting similar characteristics to diodes. However, diode-based models have unknown parameters that must be accurately identified for precise estimation. This precision is vital in controlling PV systems as the parameters change over time due to the nonlinear nature and aging of solar cells. Therefore, accurate parameter estimation techniques are essential for optimizing PV systems, ensuring maximum power extraction under different environmental conditions. Hence, research focuses on improving these techniques to enhance the performance and reliability of PV systems.

3.1. Single Diode Model (SDM)

The single-diode model (SDM) is one of the most commonly used models for simulating solar cells due to its simplicity and high usability. This model provides an equation based on the diffusion and recombination currents of the diode and includes the following elements: a current source with semiconductor material characteristics and dependence on changes in solar irradiance and cell/module temperature, a diode that models the physical effects at the p-n junction, and also a series resistance (Rs) and a shunt resistance (Rsh) for modeling ohmic losses in the semiconductor and leakage current, as shown in Figure 2.

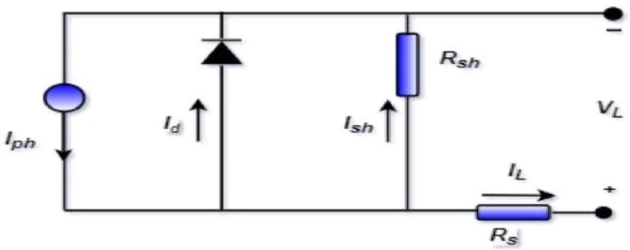

Figure 2. Equivalent circuit of a single-diode photovoltaic cell system

According to Figure 1, the output current I_L is as follows:

$$I_L = I_{ph} - I_d - I_{sh} \tag{1}$$

The shunt resistance current I_{sh} is also calculated based on the following equation:

$$I_{sh} = \frac{V_L + I_L R_S}{R_{sh}} \tag{2}$$

Furthermore, the diode current I_d is obtained using the Shockley equation as follows:

$$I_d = I_{SD}[\exp\left(\frac{q(V_L + I_L R_s)}{nkT}\right) - 1] \tag{3}$$

Finally, the equation for output current can be rewritten using the above equations as follows:

$$I_L = I_{ph} - I_{SD}\left[\exp\left(\frac{q(V_L + I_L R_s)}{nkT}\right) - 1\right] - \frac{V_L + I_L R_S}{R_{sh}} \tag{4}$$

Therefore, the SDM has five unknown parameters $\theta = [I_{ph} \ \ R_s \ \ R_{sh} \ \ I_{SD} \ \ n]$ that need to be accurately estimated.

3.2. Double-diode model (DDM)

Double-diode model (DDM) consists of two diodes in parallel with a current source, which more accurately describes the physical effects of the p-n junction, especially at low illumination levels. One diode models the junction's diffusion current, while the other diode represents the recombination effects in the space charge region. The equivalent circuit of DDM is depicted in Figure 3.

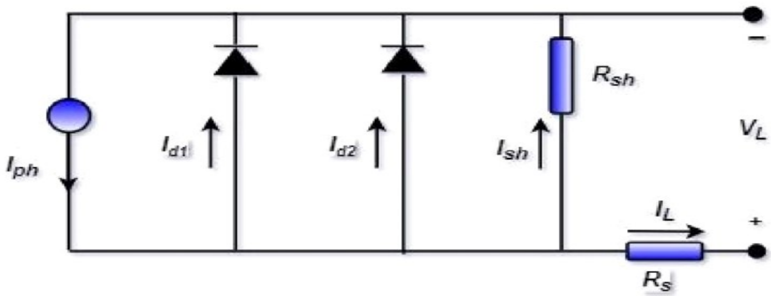

Figure 3. Equivalent circuit of the DDM model

According to Figure 2, I_{SD1} and I_{SD2} represent the diffusion and saturation currents respectively, while n_1 and n_2 are the ideality factors for the diodes.

Based on the equivalent circuit of the DDM model, the output current can be expressed as:

$$I_L = I_{ph} - I_{d_1} - I_{d2} - I_{sh} \tag{5}$$

By rewriting the above equation using a similar method to the SDM, the equation becomes:

$$I_L = I_{ph} - I_{SD1}\left[\exp\left(\frac{q(V_L + I_L R_s)}{n_1 kT}\right) - 1\right] - I_{SD2}\left[\exp\left(\frac{q(V_L + I_L R_s)}{n_2 kT}\right) - 1\right] - \frac{V_L + I_L R_S}{R_{sh}} \quad (6)$$

Therefore, this model has seven unknown parameters, which can be expressed as the vector

$$\theta = [I_{ph}\ R_s\ R_{sh}\ I_{SD_1}\ I_{SD_2}\ n_1\ n_2] \quad (7)$$

4. RESULTS AND DISCUSSION

The Results and Discussion section delves into the analysis of data obtained from experiments utilizing the GOA for parameter estimation in PV solar cells and modules. The findings reveal that the proposed GOA methodology surpasses other meta-heuristic algorithms like WOA, GWO, HHO, AVOA, and COA in effectively reducing Root Mean Square Error (RMSE) and standard deviation across Single-Diode Model (SDM), Double-Diode Model (DDM), and PV modules. Figure 4 presents a visual representation of algorithm rankings based on minimal RMSE error.

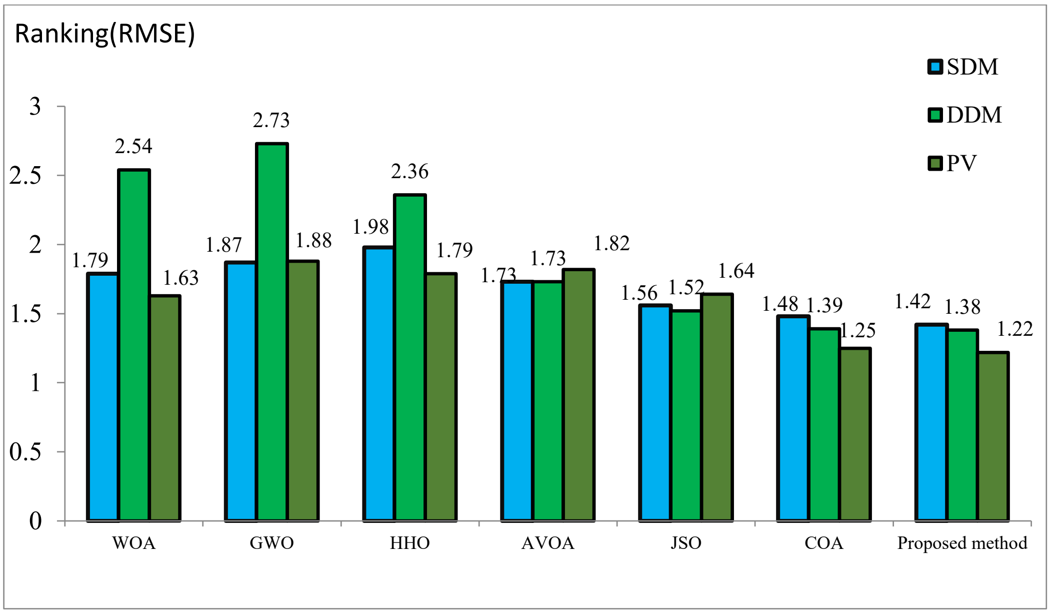

Figure 4. Ranking of algorithms in calculating the minimum RMSE error

The GOA algorithm emerges as the top performer in parameter optimization for SDM, DDM, and PV circuits, showcasing its superior accuracy in estimating model parameters compared to rival algorithms. Furthermore, a comparison with the COA algorithm highlights a significant enhancement in optimal calculation rank across all three circuits. In Figure 5, the average rank of the proposed algorithm and other meta-heuristic algorithms is depicted using the standard deviation index. This index is pivotal for assessing the stability of optimization algorithms in parameter optimization for SDM, DDM, and PV circuits. The results demonstrate that the GOA algorithm achieves a commendable average standard deviation in all three modes, underscoring its stability and robustness in parameter estimation. In conclusion, the data analysis validates the efficacy and practical utility of the GOA algorithm for parameter estimation in PV solar cells and modules. The outstanding performance of this methodology in error reduction and model parameter optimization highlights its potential to drive advancements in renewable energy technologies and foster sustainable development in solar power generation. These results offer compelling evidence in favor of adopting the GOA algorithm as a dependable tool for enhancing the performance and efficiency of photovoltaic systems.

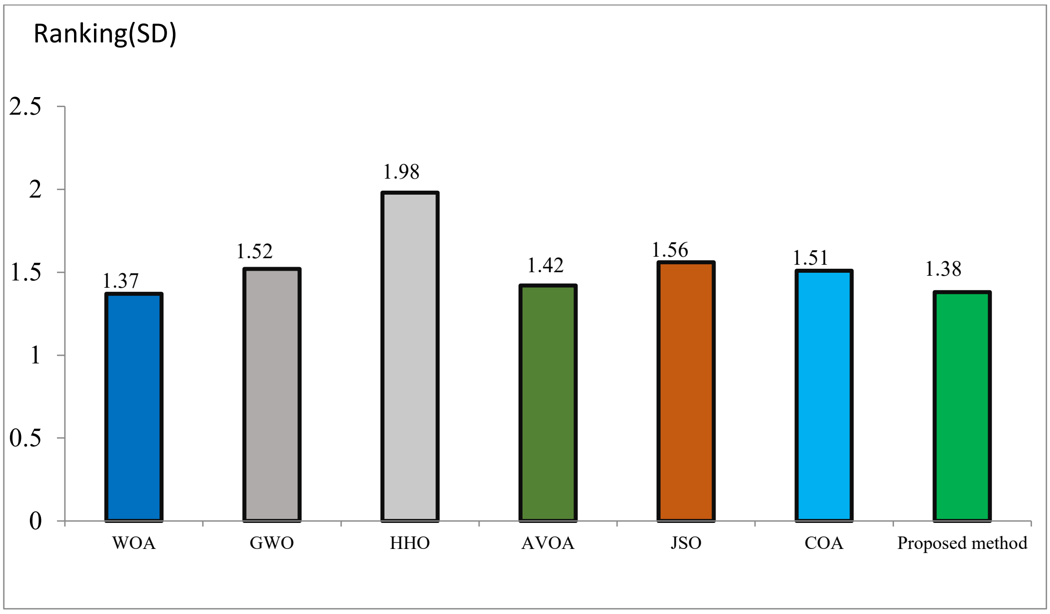

Figure 5: Algorithm ranking based on standard deviation (SD) index

5. CONCLUSION

Photovoltaic (PV) solar cells and modules are crucial components in the renewable energy sector, emphasizing the importance of precise parameter estimation to enhance their effectiveness and efficiency. This research advocates for utilizing the GOA as a robust tool for parameter estimation in PV solar cells and modules. The methodology proposed aims to improve the accuracy and efficacy of parameter estimation by leveraging the unique search mechanism of the GOA, inspired by the foraging behavior of grasshoppers in nature. Through iterative optimization of the solution space, the GOA efficiently explores various possibilities to identify optimal parameters that closely match experimental data, including current-voltage (IV) and PV characteristics. The study meticulously outlines the parameter estimation process, explaining the formulation of an objective function that minimizes the differences between experimental and simulated data. Additionally, it discusses the implementation of the GOA algorithm and its seamless integration with mathematical models of PV solar cells and modules. Validation of the proposed approach involves using real-world experimental data from PV systems. Comparative analyses with other optimization algorithms highlight the superior performance of the GOA in terms of convergence speed and precision in parameter estimation. The results emphasize that this methodology provides a robust and efficient solution for parameter estimation in PV solar cells and modules, streamlining the design, optimization, and maintenance of photovoltaic systems. The integration of the GOA algorithm represents a significant advancement in renewable energy technologies, promoting the widespread adoption of solar power generation for sustainable development. This paper underscores the practical applicability and effectiveness of the Grasshopper Optimization Algorithm for parameter estimation in PV solar cells and modules. By providing accurate model parameters, the proposed methodology facilitates progress in renewable energy technologies and advocates for the extensive incorporation of solar power to promote sustainability.

REFERENCES

[1] A. Rauf, N. Nureen, M. Irfan, and M. Ali, "The current developments and future prospects of solar photovoltaic industry in an emerging economy of India," *Environ. Sci. Pollut. Res.*, vol. 30, no. 16, pp. 46270–46281, 2023.

[2] Z. Yusupov, N. Almagrahi, E. Yaghoubi, E. Yaghoubi, A. Habbal, and D. Kodirov, "Modeling and Control of Decentralized Microgrid Based on Renewable Energy and Electric Vehicle Charging Station," in *World Conference Intelligent System for Industrial Automation*, 2022, pp. 96–102.

[3] X. Wu, B. Liao, Y. Su, and S. Li, "Multi-objective and multi-algorithm operation optimization of integrated energy system considering ground source energy and solar energy," *Int. J. Electr. Power Energy Syst.*, vol. 144, p. 108529, 2023.

[4] Z. Yusupov, E. Yaghoubi, and V. Soyibjonov, "REDUCING THE VULNERABILITY IN MICROGRID POWER SYSTEMS," *Sci. Innov.*, vol. 2, no. A5, pp. 166–175, 2023.

[5] A. S. Irshad, "Design and comparative analysis of grid-connected BIPV system with monocrystalline silicon and polycrystalline silicon in Kandahar climate," in *MATEC Web of Conferences*, 2023, vol. 374, p. 3002.

[6] N. Balamurugan, P. Karuppasamy, and P. Ramasamy, "Investigation on different crystal grains from the multi-crystalline silicon (mc-Si) wafer," *Silicon*, vol. 15, no. 3, pp. 1465–1474, 2023.

[7] S. Kar, S. Banerjee, and C. K. Chanda, "Performance study of Amorphous-Si thin-film solar cell for the recent application in photovoltaics," *Mater. Today Proc.*, vol. 80, pp. 1286–1290, 2023.

[8] S. B. Hamed *et al.*, "A robust MPPT approach based on first-order sliding mode for triple-junction photovoltaic power system supplying electric vehicle," *Energy Reports*, vol. 9, pp. 4275–4297, 2023.

[9] P. K. Bonthagorla and S. Mikkili, “A Novel Hybrid Slime Mould MPPT Technique for BL-HC Configured Solar PV System Under PSCs,” *J. Control. Autom. Electr. Syst.*, pp. 1–14, 2023.
[10] S. C. Nwokolo, A. U. Obiwulu, and J. C. Ogbulezie, “Machine learning and analytical model hybridization to assess the impact of climate change on solar PV energy production,” *Phys. Chem. Earth, Parts A/B/C*, vol. 130, p. 103389, 2023.
[11] A. D. Tuncer *et al.*, “Experimental and numerical analysis of a grooved hybrid photovoltaic-thermal solar drying system,” *Appl. Therm. Eng.*, vol. 218, p. 119288, 2023.
[12] Y. Zhang, Y. Wu, L. Li, and Z. Liu, “A Hybrid Energy Storage System Strategy for Smoothing Photovoltaic Power Fluctuation Based on Improved HHO-VMD,” *Int. J. Photoenergy*, vol. 2023, 2023.